Integration of a Resonant Tunneling Diode and an Optical Communications Laser

T. J. Slight, C. N. Ironside, *Senior Member, IEEE*, C. R. Stanley, M. Hopkinson, and C. D. Farmer

***Abstract*—We report on the first integration of a resonant tunneling diode and an optical communications laser operating at around 1.5 μm. We demonstrate its low-frequency bistable operation and model its electrical characteristics.**

***Index Terms*—Driver circuits, integrated optoelectronics, optical bistability, optical fiber communication, resonant tunneling diodes (RTDs), semiconductor lasers.**

I. Introduction

In THIS letter, we demonstrate the use of a resonant tunneling diode (RTD) as a driver for a semiconductor laser. This is a novel alternative to traditional transistor-based driver circuits [1]. The RTD acts as a voltage controlled switch for the laser and causes the device (the RTD-LD) to become electrically bistable, making it particularly convenient for nonreturn-to-zero (NRZ) digital modulation. Digital signals with low power can be employed to switch the device between ON and OFF states and the high-speed modulation characteristics of the laser will be improved by the smaller drive powers required. Furthermore, integration of a RTD fits well with the vertical stack arrangement of the epitaxial layers that make up a semiconductor laser, and so it is easily achieved by introducing two barrier layers close to the contact layer.

Previous light emitting devices utilizing the resonant tunneling diode/effect include the resonant tunneling light-emitting diode (RTLED) [2], the resonant tunneling effect quantum well laser [3], and the resonant tunneling injection laser [4]. Grave *et al.* [5] have demonstrated an integrated RTD/laser in the GaAs–AlGaAs material system and have demonstrated its application as an optical two state memory. In this work, we are targeting optical communications applications with the emphasis on increased functionality and an emission wavelength of around 1.55 μm. We have characterized the low-frequency operation of the RTD-LD, demonstrated optical/electrical bistability, and modeled its electrical characteristics using SPICE [6].

II. Device Layout

A suitable wafer for the device was grown by molecular beam epitaxy and consisted of a resonant tunneling diode grown above a multiple quantum well laser. This vertical integration of RTD and laser is straightforward as the RTD section requires only three extra epilayers of growth in addition to the basic laser structure.

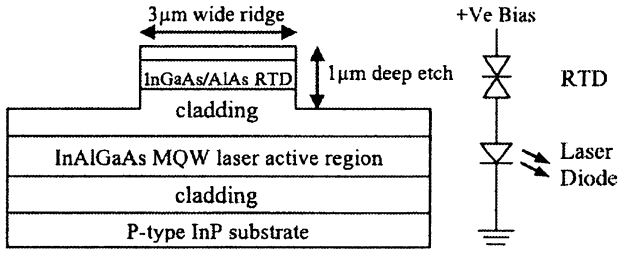

Fig. 1. Cross section (not to scale) of layout of ridge waveguide RTD laser. Cavity length is 500 μm, giving an RTD active area of 1500 μm^2. Alongside is schematic circuit representation of device.

The laser section was based on a design presented in [7] and consisted of six 6.7-nm-thick InGaAs quantum wells with 10-nm InGaAlAs barriers. The RTD consisted of a 5-nm InGaAs quantum well sandwiched by strained 2-nm AlAs barriers. Devices were fabricated based on the ridge waveguide laser design shown in Fig. 1. In order to control its active area, the RTD was situated in the waveguiding ridge, between the laser section of the device and the n-type contact. The laser had a cavity length of 500 μm, and so with the 3-μm ridge width the RTD had an active area of 1500 μm^2. The laser active area was a minimum of 1500 μm^2 with the actual area dependent on the extent of current spreading beneath the ridge. RTDs usually operate with n-type material, and therefore in this design it was more convenient to use a p-type InP substrate.

III. Principles of Operation

To understand how the series combination of RTD and laser will behave electrically and optically, it is worthwhile to consider the graphical technique of load line analysis. This method is used to determine the operating point of the series combination of two devices. The current–voltage characteristic of one device is plotted on the same axes as the load line of the second. The load line is simply the current through the second device as a function of the voltage across the first. The point where the load line intersects the current–voltage characteristic gives the operating point of the series combination.

Fig. 2 illustrates the principles of operation of the RTD-LD using the load line technique. The bold plot gives a simulated current–voltage characteristic for a RTD, which was based on a model presented in [8]. The RTD exhibits negative differential resistance (NDR), i.e., as the RTD voltage rises above a threshold value (V_{peak}) the RTD current drops steeply from its

Manuscript received February 16, 2006; revised April 12, 2006. The work of T. J. Slight was supported by the Engineering and Physical Sciences Research Council (EPSRC).

T. J. Slight, C. N. Ironside, C. R. Stanley, and C. D. Farmer are with the Department of Electronics and Electrical Engineering, University of Glasgow, Glasgow G12 8LT, U.K.

M. Hopkinson is with the Department of Electronic and Electrical Engineering, University of Sheffield, Sheffield, U.K.

Digital Object Identifier 10.1109/LPT.2006.877574

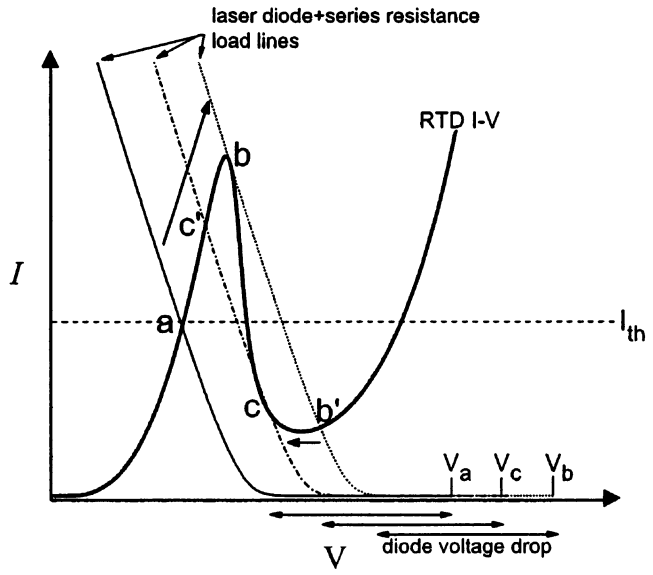

Fig. 2. Illustration using load line analysis to explain operation of series combination of RTD and laser diode. Bold plot represents I–V characteristic of RTD, and three lines represent load lines of laser diode with series resistance at three different bias voltages. Dashed horizontal line represents laser threshold current.

peak value (I_{peak}) to a lower value (I_{valley}) before rising again. The RTD current–voltage characteristic is overlaid with a horizontal line to represent the laser threshold current (I_{th}) (the condition $(I_{\text{peak}} > I_{\text{th}} > I_{\text{valley}})$ needs to be met for the device to operate as described) and three load lines to represent the laser diode combined with any series resistance R_s attributable to the laser diode itself or the external circuit (one load line for each of three different bias voltages—V_a, V_b, and V_c). The load line illustrates the diode voltage drop followed by a period of exponential growth before tending to the gradient $1/R_s$.

When the bias voltage is increased from 0 V to V_a, the load line will reach point (a) upon which the current will reach I_{th} and the laser will switch on. As the voltage increases further to V_b, the load line will reach point (b) and the current will jump from point (b) to point (b') below I_{th} and the laser will switch off. Now decreasing the voltage to V_c will cause the current to jump from point (c) to point (c') and the laser will switch on again. Clearly, the current–voltage characteristic will differ depending on whether the voltage is increasing or decreasing, resulting in electrical/optical hysteresis in the device. This hysteresis occurs if (as in this example) the load line slope $(-1/R_s)$ is not as steep as the NDR region of the RTD current–voltage characteristic. Lower values of series resistance would reduce and eventually remove the hysteresis.

IV. Results and Discussion

The dc electrical and optical characteristics of the device are shown in Figs. 3 and 4. For epilayer up mounting of the RTD-LD, to obtain cw laser operation, it was necessary to operate the device at a temperature of 130 K. We anticipate with some improvement of the laser design and epilayer down mounting, room temperature operation will be obtainable.

From Fig. 3, we can see that the device is electrically bistable and thereby optically bistable, confirmed by Fig. 4.

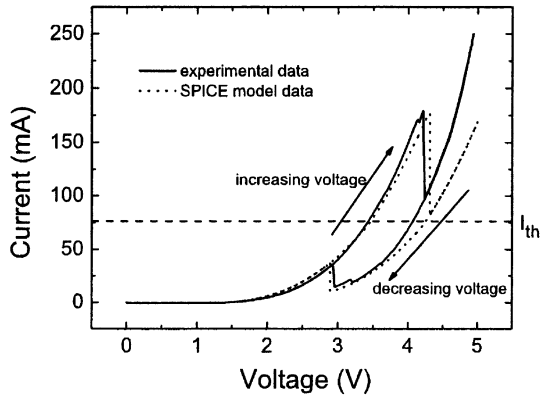

Fig. 3. Current versus voltage curve for RTD-LD at 130 K showing clear hysteresis and electrical bistability. Dashed horizontal line represents threshold current of laser. With RTD active area of 1500 μm^2, RTD peak and valley current densities are 11947 and 980 $A\text{cm}^{-2}$ respectively, giving a peak-to-valley current ratio of 12. SPICE model data is given by dotted curves.

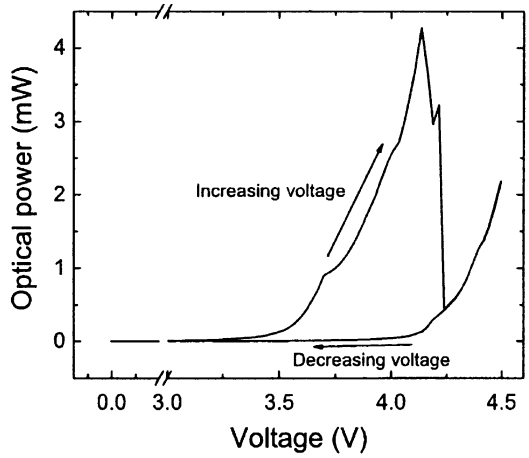

Fig. 4. Optical power versus voltage curve for RTD-LD at 130 K showing hysteresis and bistability.

The threshold current of the laser is represented by a dashed line in Fig. 3 and was taken from the optical power versus current curve in Fig. 5. The width of the hysteresis loop is 1.3 V and so when dc biased to the middle of the loop a +0.65-V pulse will switch the laser from ON to OFF states and a −0.65-V will switch the laser from OFF to ON states. There is an optical extinction ratio of 20 dB between the two states, so a 0.65-V pulse can provide 20 dB of modulation. Furthermore, with a bistable device NRZ modulation is more easily obtained.

Bistability in RTDs can arise for one of two reasons. The intrinsic bistability—where charge storage allows two different states of band bending for one applied bias—has been observed by Alves *et al.* [9] and explained theoretically in [10] and [11]. The extrinsic bistability is illustrated in the load line analysis of Fig. 2 and is caused by the presence of the laser diode and series resistance.

SPICE, the general purpose analog circuit simulator, was used to model the RTD-LD and show whether the observed bistability in Figs. 3 and 4 is explainable in terms of the extrinsic effect. The SPICE RTD model presented by Brown [8] was modified to replicate the observed peak and valley RTD currents of the RTD-LD. A simple diode model was used to

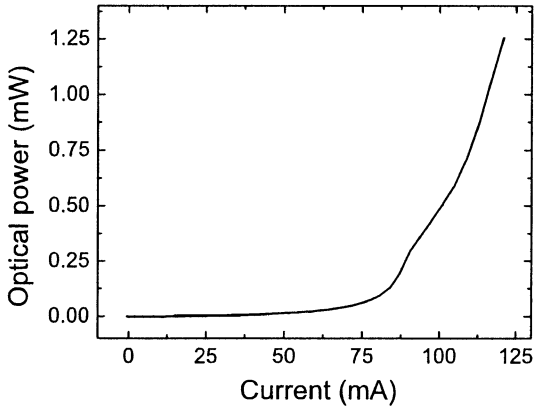

Fig. 5. Optical power output versus drive current for RTD-LD at 130 K. Laser threshold current is 77 mA.

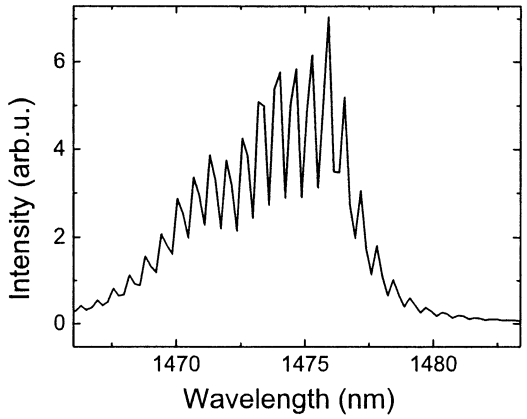

Fig. 6. Emission spectrum of RTD-LD at 130 K (0.2-nm resolution).

represent the electrical characteristics of the laser diode. Using a method presented in [12], whereby the gradient of the RTD I-V characteristic is measured at higher biases as it tends to the value $1/R_s$, the series resistance of the RTD-LD was found to be 3 Ω. This series resistance was added to the simulation. After adjusting the diode model parameters of saturation current and ideality factor, the best fit obtainable with the SPICE RTD-LD model is given in Fig. 3. The fit agrees with the experimental data at low voltages but fails to replicate the increase in current as the bias increases above $V_{\rm peak}$. This is a consequence of the RTD model I–V not matching the the actual device RTD section I–V at biases above $V_{\rm peak}$. The experimental hysteresis widths of the RTD-LD (1.3 V) could be replicated in the SPICE model and therefore the RTD-LD optical/electrical bistability was attributed to the extrinsic load line effect of the laser diode and series resistance.

The optical spectrum at 130 K for the device is given in Fig. 6; the central peak is at a wavelength of 1.476 μm. The RTD-LD operated as a laser at room temperature with a pulsed drive current, and under these conditions the emission wavelength was 1.54 μm. The 130 K operating temperature shifted the emission peak to a shorter wavelength.

The device can be improved by refinement of the laser section design in combination with epilayer down mounting to enable room temperature operation and a lower threshold current. In addition, decreasing $I_{\rm peak}$ and $I_{\rm valley}$ with an improved RTD design will reduce the hysteresis width according to the simulation results and match a lowered laser threshold current. The reduced hysteresis loop width will lower the voltage of drive signals required by the device. Further investigation of the RTD-LD will include characterizing the high-speed operation.

REFERENCES

[1] P. R. Berger, N. K. Dutta, D. L. Sivco, and A. Y. Cho, "GaAs quantum-well laser and heterojunction bipolar-transistor integration using molecular-beam epitaxial regrowth," *Appl. Phys. Lett.*, vol. 59, no. 22, pp. 2826–2828, 1991.

[2] C. Vanhoof, J. Genoe, R. Mertens, G. Borghs, and E. Goovaerts, "Electroluminescence from bipolar resonant tunneling diodes," *Appl. Phys. Lett.*, vol. 60, no. 1, pp. 77–79, 1992.

[3] Y. Kawamura, H. Asai, and H. Iwamura, "Fabrication of resonant-tunneling optical bistable laser-diodes," *Electron. Lett.*, vol. 30, no. 3, pp. 225–227, 1994.

[4] C. R. Lutz, F. Agahi, and K. M. Lau, "Resonant-tunneling injection quantum-well lasers," *IEEE Photon. Technol. Lett.*, vol. 7, no. 6, pp. 596–598, Jun. 1995.

[5] I. Grave, S. Kan, G. Griffel, S. Wu, A. Saar, and A. Yariv, "Monolithic integration of a resonant tunneling diode and a quantum-well semiconductor-laser," *Appl. Phys. Lett.*, vol. 58, no. 2, pp. 110–112, 1991.

[6] G. W. Roberts and A. S. Sedra, *SPICE*, 2nd ed. Oxford: Oxford Univ. Press, 1997.

[7] M. Jain, "An investigation of broad gain spectrum InGaAs/InAlGaAs quantum well lasers latticed matched to InP," Ph.D. dissertation, Univ. Glasgow, Glasgow, U.K., 2002.

[8] E. R. Brown, O. B. McMahon, L. J. Mahoney, and K. M. Molvar, "SPICE model of the resonant-tunnelling diode," *Electron. Lett.*, vol. 32, no. 10, pp. 938–940, 1996.

[9] E. S. Alves, L. Eaves, M. Henini, O. H. Hughes, M. L. Leadbeater, F. W. Sheard, G. A. Toombs, G. Hill, and M. A. Pate, "Observation of intrinsic bistability in resonant tunnelling devices," *Electron. Lett.*, vol. 24, no. 18, pp. 1190–1191, 1988.

[10] F. W. Sheard and G. A. Toombs, "Space-charge buildup and bistability in resonant-tunneling double-barrier structures," *Appl. Phys. Lett.*, vol. 52, no. 15, pp. 1228–1230, 1988.

[11] M. Rahman and J. H. Davies, "Theory of intrinsic bistability in a resonant tunneling diode," *Semiconductor Sci. Technol.*, vol. 5, no. 2, pp. 168–176, 1990.

[12] M. J. Deen, "Simple method to determine series resistance and its temperature-dependence in AlAs/GaAs/AlAs double barrier resonant tunneling diodes," *Electron. Lett.*, vol. 28, no. 13, pp. 1195–1197, 1992.